



**HAL**  
open science

# Dynamics of Cylindrical and Spherical Objects on a Turntable

Kyeong Min Kim, Donggeon Oh, Junghwan Lee, Young-Gui Yoon,  
Chan-Oung Park

► **To cite this version:**

Kyeong Min Kim, Donggeon Oh, Junghwan Lee, Young-Gui Yoon, Chan-Oung Park. Dynamics of Cylindrical and Spherical Objects on a Turntable. 2018. hal-01761333

**HAL Id: hal-01761333**

**<https://hal.science/hal-01761333>**

Preprint submitted on 9 Apr 2018

**HAL** is a multi-disciplinary open access archive for the deposit and dissemination of scientific research documents, whether they are published or not. The documents may come from teaching and research institutions in France or abroad, or from public or private research centers.

L'archive ouverte pluridisciplinaire **HAL**, est destinée au dépôt et à la diffusion de documents scientifiques de niveau recherche, publiés ou non, émanant des établissements d'enseignement et de recherche français ou étrangers, des laboratoires publics ou privés.

# Dynamics of Cylindrical and Spherical Objects on a Turntable

Kyeong Min Kim<sup>\*</sup>, Donggeon Oh<sup>‡</sup>, Junghwan Lee<sup>†</sup>,  
Young-Gui Yoon<sup>§</sup>, Chan-Oung Park<sup>¶</sup>

<sup>\*</sup> *Department of Physics, University of Oxford, Oxford, United Kingdom*

<sup>\* †</sup> *Cheongshim International Academy, Gyeonggi-do, South Korea*

<sup>‡</sup> *Department of Aerospace Engineering, Seoul National University, Seoul, South Korea*

<sup>‡</sup> *Gyeonggi Science High School for the Gifted, Gyeonggi-do, South Korea*

<sup>§</sup> *Department of Physics, Chung-Ang University, Seoul, South Korea*

<sup>¶</sup> *Department of Nanophysics, Gachon University, Gyeonggi-do, South Korea*

## Abstract

A circular object placed on a rotating turntable demonstrates an interesting motion. Such motion consists of the rolling object exhibiting a spiral motion with increasing radius and the center of the spiral drifting towards the center of the turntable. This paper suggests a novel approach to the dynamics of the motion when the contact between the cylindrical rolling object and the turntable is a line. Under an assumption that the rolling objects contact point with the turntable is quasistatic, this paper approximates a theoretical model to solve for the maximum radius of the spiral orbit and the frequency of such circular motion. The theoretical model will include the effect of various parameters on the motion, such as, the coefficient of rolling friction, the coefficient of kinetic friction, the coefficient of pivoting friction and the geometry of the rolling object.

## I. INTRODUCTION

The motion of a rolling object, when placed on a rotating turntable, is complicated at first sight, but analyzable. Some authors<sup>1-5</sup> proved that the ball would execute a constant circular motion, under the assumption that the static friction is applied to the ball. However, this assumption cannot be held accountable for experimental results because the presence of kinetic friction is inevitable on a rapidly rotating turntable. Through this realistic approach, Weltner proved the center of the circular motion of the ball drifts towards the center of the turntable due to the presence of rolling friction<sup>2</sup>, and Ehrlich solved the ball will follow a certain circular trajectory with gradually increasing radii when the ball slips<sup>6</sup>. As depicted by Fig. 1, the objects draw a spiral trajectory.

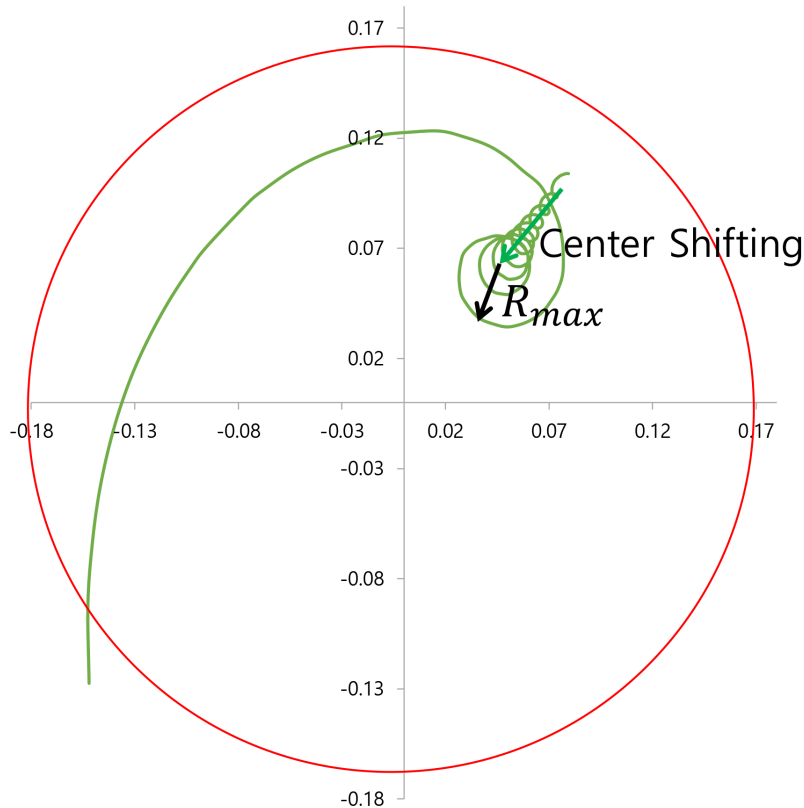


FIG. 1: Explanation of the motion of the rolling object : description of variable  $R_{max}$ , the maximum radius of the non-slipping stage, and the movement of the rolling object towards the center of the turntable.

Ehrlich extended the analysis of the balls motion by exploring the transition between

rolling with and without slipping.<sup>6</sup> Before the transition from a non-slip condition to a slipping condition, the ball continues the spiral (divergent) motion in constant frequency. However, after the transition, the frequency of the motion changes and the ball notably slips.

Although the contact part between the ball and the turntable is a point, the contacting region between the cylindrical rolling objects, such as a ring or a disc, and the turntable is a line. In addition, the discs have fixed axis of rotation. Therefore, the motion of the disc is far more complicated than the motion of the ball. Some authors studied about the dynamics of the rolling and sliding discs on a non-rotating surface.<sup>9-13</sup> Also, previous researches handled the energy dissipation of the disc due to the pivoting friction.<sup>14-17</sup> Pivoting friction applies torque at the opposite direction of the z axis rotation to decrease the z axis angular momentum.

Moreover, while preceding researches are focused on the rolling object on a turntable as a ball or just a simple motion of a disc, such as its rotation and precession on a fixed surface, we also analyzed the motion of a disc and a ring as a rolling object on a turntable. The various geometry of the rolling object was then taken into account with the normalized moment of inertia to explicate the motion of the different rolling objects.

In addition, previous research papers<sup>1-8</sup> lack the quantitative experimental verification of their theoretical model. One paper<sup>6</sup> does contain qualitative data obtained from simulations, but only to a certain limit where it cannot be thoroughly compared in contrast to the observed motion.

In order to verify the theory, and for a firm grasp of the idea of the motion itself, this paper corroborates the theoretical approach through experiments, unlike preceding researches. The measured variables chosen to be researched in this paper are the frequency of the objects circular motion and the maximum radius of the objects orbit (refer to Fig. 1), which varies under change of the geometry of the object, the frequency of the turntable, and the coefficient of friction. The maximum radius of the orbit is the radius of the circular motion just before the transition into the slipping stage. Reasons for such variance will be elaborated in the following sections.

## II. THE EQUATIONS OF MOTION

We derive the equations of motion about the rolling object on a turntable rotating at a constant frequency. Two theoretical models describe two different motions:

(A) Model that describe the motion of the rolling object with a contact point, such as a ball or a sphere.

(B) Model that describe the motion of the rolling object with a contact line, such as a ring, a disc, or a cylinder.

The suggested models (A) and (B) refer to kinetic friction model for contact point and kinetic friction model for contact line.

### A. Kinetic Friction Model for Contact Point

In order to analyze the motion of the rolling object in the presence of kinetic friction, we derive the equations of motion in an inertial frame of reference with its origin at the center of the turntable. The kinetic friction acts to decrease the momentum of the contact point between the rolling object and the turntable.

The equation of the motion of the center of mass is written as

$$\sum \vec{F} = m\vec{v}_f = -\mu mg\hat{v}_{re} \quad (1)$$

The relative velocity between the bottom of the rolling object and the surface of the turntable is expressed as

$$\vec{v}_{re} = \vec{v}_f + \omega \times (-a\hat{k}) - \Omega\hat{k} \times \vec{r} \quad (2)$$

The kinetic friction in this system also produces a torque about the center of mass of the rolling object. The torque produced by kinetic friction is

$$\vec{\tau}_k = (-a\hat{k}) \times (-\mu mg\hat{v}_{re}) \quad (3)$$

In addition to kinetic friction, this model considers the rolling friction. The rolling friction is caused by three factors: the deformation of the rolling object, the collision of micro-level bumps between the rolling object and the turntable, and the adhesion between the rolling object and the turntable.<sup>5</sup> The torque created by rolling friction is assumed to decrease the

TABLE I: Summary of nomenclature

$\vec{r}$	Position vector of the rolling object
$l$	Rotational axis of the rolling object parallel to xy plane
$\vec{v}_f$	Velocity in fixed coordinate
$\vec{v}_r$	Velocity in rotational coordinate
$\vec{v}_{re}$	Relative velocity between a point at the bottom of the rolling object and the turntable
$m$	Mass of the rolling object
$\rho$	Density of the rolling object
$a$	Radius of the rolling object
$\theta_z$	Z axis angular displacement(Angle between $\hat{l}$ and $\hat{x}$ )
$\vec{\omega}$	Angular velocity of the rolling object
$\vec{\omega}_z$	Z axis angular velocity of the rolling object
$I$	Moment of inertia of the rolling object
$I_l$	Moment of inertia of the rolling object about $l$ axis
$I_z$	Moment of inertia of the rolling object about $z$ axis
$I'$	Normalized Moment of inertia of the rolling object
$\Omega$	Magnitude of angular velocity of the turntable
$\hat{k}$	Unit vector pointing upward from the turntable
$\mu$	Coefficient of kinetic friction
$g$	Gravitational acceleration
$\beta$	Coefficient of rolling friction
$k$	Coefficient of pivoting friction

angular momentum of the rolling object with a constant magnitude. The rolling friction torque is then defined as

$$\vec{\tau}_r = -\beta m g a \hat{\omega} \quad (4)$$

Therefore, the dynamic equation for the rotation of the rolling object is written as

$$\sum \vec{\tau} = I \vec{\omega} = \left(-a \hat{k}\right) \times \left(-\mu m g v_{re}\right) - \beta m g a \hat{\omega} \quad (5)$$

By rearranging Eq. (1) and Eq. (5), we get two final equations as below

$$\vec{v}_f = -\mu g v_{re} \hat{e}_r \quad (6)$$

$$\vec{\omega} = \frac{\mu m g a \hat{k} \times v_{re} - \beta m g a \hat{\omega}}{I} \quad (7)$$

In addition to the kinetic friction model, we can analyze the divergent motion using the characteristics of the contact point between the rolling object and the turntable. This paper defines a divergent motion as a spiral motion with an increasing radius. When the rolling object is in its non-slipping stage, the objects contact point is during its divergent motion.<sup>6</sup> Then the velocity of the rolling object with a quasistatic contact point is expressed as

$$v_{rel}^{\vec{v}} = \vec{\omega} \times a \hat{k} (1 + \delta) + \Omega \hat{k} \times \vec{r} \approx \vec{\omega} \times a \hat{k} + \Omega \hat{k} \times \vec{r} \quad (8)$$

where  $\delta$  is an infinitesimal. With Eq. (8) we could approximate the spiral motion of the rolling object as a quasicircular motion with a quasistatic contact point. With this approximation, the model explains the frequency of the circular spiral motion of the rolling object and the maximum radius of the orbit, the radius of the circular orbit just before the transition to the slipping stage.

By substituting Eq. (6) in Eq. (7), we obtain

$$\vec{\omega} = \frac{a m \hat{k} \times \vec{v}_f - \beta m g a \hat{\omega}}{I} \quad (9)$$

Because the magnitude of torque produced by rolling friction is negligible compared to the magnitude of torque produced by kinetic friction, we approximate  $\vec{\omega}$  as

$$\vec{\omega} = \frac{a m \hat{k} \times \vec{v}_f}{I} \quad (10)$$

Combining Eq. (10) and the time derivative of Eq. (8) ( $\vec{v}_f \approx \vec{\omega} \times a \hat{k} + \Omega \hat{k} \times \vec{v}_f$ ), we obtain the equation of the motion

$$\frac{I + m a^2}{I} \vec{v}_f - \Omega \hat{k} \times \vec{v}_f = 0 \quad (11)$$

In this phenomenon of an object rolling on a turntable, the moment of inertia does not give the true information about the geometry of the object. On that account, we introduce a new variable, normalized moment of inertia  $I'$ , which is defined as follows:

$$I' = \frac{I}{m a^2} \quad (12)$$

By arranging Eq. (11) about  $\vec{v}_f$  and substituting Eq. (12), we get the equation of motion in terms of the normalized moment of inertia as

$$\vec{v}_f = \frac{I'}{I' + 1} \Omega \hat{k} \times \vec{v}_f \quad (13)$$

Eq. (13) is an equation of a circular motion with angular velocity

$$\Omega' = \frac{I'}{I' + 1} \Omega \quad (14)$$

If we denote the maximum radius of the orbit as  $R_{max}$ , the transition between the non-slipping stage and the slipping stage occurs when centrifugal force equates to the kinetic friction force as

$$m\Omega'^2 R_{max} = \mu mg \quad (15)$$

By arranging Eq. (15) about  $R_{max}$  and substituting Eq. (14), we attain the general equation about  $R_{max}$

$$R_{max} = \mu g \left( \frac{I' + 1}{I' \Omega} \right)^2 \quad (16)$$

## B. Kinetic Friction Model for Contact Line

We derive the equations of motion in an inertial frame of reference with its origin at the center of the turntable. To analyze the motion of the cylindrical rolling object with a contact line on the turntable, such as disc, ring, or cylinder, we derive the force equation, the net torque about the  $l$  axis and the net torque equation about the  $z$  axis. Because the contact part between the rolling object and the turntable is a line, the direction of the kinetic friction is different for each part of the contact points. Therefore, we should consider each infinitesimal parts,  $dm$ , of the disc to calculate the kinetic friction force.

The kinetic friction force is

$$\vec{F} = m\vec{v}_f = \int d\vec{F} = - \int \mu g v_{re} \hat{e} dm = - \int_{-d/2}^{d/2} \mu g \rho \pi a^2 v_{re} \hat{e} dl \quad (17)$$

Considering the  $z$  axis rotation, the relative velocity between a point on the contact line and the surface of the turntable is expressed as

$$v_{re} = \vec{v}_f + \vec{\omega} \times (-a\hat{k}) - \Omega \hat{k} \times (\vec{r} + \vec{l}) + \vec{\omega}_z \times \vec{l} \quad (18)$$

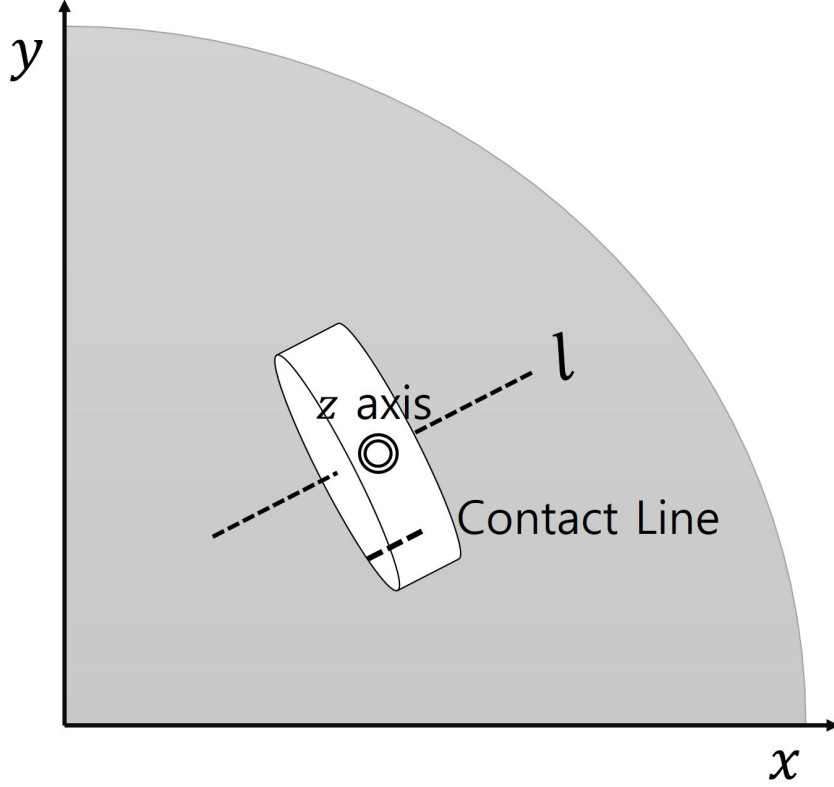


FIG. 2: Explanation of the system of disc rolling on the turntable: description of  $l$  axis,  $z$  axis, and contact line.

or using unit vectors, the relative velocity can also be expressed as

$$\begin{aligned} \vec{v}_{re} = & (\dot{x} - l\omega_z \sin \theta_z - a\omega \sin \theta_z + (y + l \sin \theta_z) \Omega) \hat{i} \\ & + (\dot{y} + l\omega_z \cos \theta_z + a\omega \cos \theta_z - (x + l \cos \theta_z) \Omega) \hat{j} \end{aligned} \quad (19)$$

The kinetic friction and rolling friction applied on the object also produce the torque about the  $l$  axis. Because we only account for the rotation about  $l$  axis in this torque equation, the torque is produced by the component of the force perpendicular to  $l$  axis. The equation of the net torque about the  $l$  axis can be modeled as

$$\begin{aligned} \sum \vec{\tau} = I_l \vec{\omega} = & (-a\hat{k}) \times (\hat{l} \times \vec{F} \times \hat{l}) - \beta m g a \hat{\omega} \\ = & (-a\hat{k}) \times \left( \hat{l} \times \left( - \int_{-d/2}^{d/2} \mu g \rho \pi a^2 v_{re} \hat{l} dl \right) \times \hat{l} \right) - \beta m g a \hat{\omega} \end{aligned} \quad (20)$$

or using trigonometry, net torque equation about  $l$  axis can also be expressed as

$$\sum \vec{\tau} = a m v_f \sin \left( \arctan \frac{\ddot{y}}{\ddot{x}} - \theta_z \right) \hat{l} - \beta m g a \hat{\omega} \quad (21)$$

In addition, the kinetic friction and pivoting friction torque applied on the object produce the torque about the  $z$  axis. The torque produced by kinetic friction is expressed as

$$\vec{\tau} = I_z \vec{\dot{\omega}} = \int \vec{l} \times d\vec{F} = - \int_{-d/2}^{d/2} \vec{l} \times \mu g \rho \pi a^2 \hat{v}_{re} dl \quad (22)$$

According to the results of previous studies<sup>16,17</sup>, the pivoting friction is approximately defined as

$$\tau_p = -kmg\hat{\omega}_z \quad (23)$$

Therefore, the net torque equation of  $z$  axis is written as

$$\tau_z = I_z \vec{\dot{\omega}}_z = - \int_{-d/2}^{d/2} \vec{l} \times \mu g \rho \pi a^2 \hat{v}_{re} dl - kmg\hat{\omega}_z \quad (24)$$

or using trigonometry, the net torque equation of  $z$  axis can be expressed as

$$\sum \vec{\tau}_z = - \left( \int_{-d/2}^{d/2} l \mu g \rho \pi a^2 |v_{re}| \sin \left( \arctan \frac{\ddot{y}}{\ddot{x}} - \theta_z \right) dl \right) \hat{z} - kmg\hat{\omega}_z \quad (25)$$

By combining Eq. (17), Eq. (21), Eq. (25), we can solve for the motion of the rolling object with contact line on the turntable.

Using the equations of the motion, we can analyze the divergent motion of the rolling object with a contact line. We assume that the rolling object is quasistatic during its divergent motion and the rolling object is thin enough to suppose that the kinetic friction applied on each points on the contact line has a consistent direction. Because the direction of the kinetic friction on each points is consistent, the net torque about  $z$  axis is negligible, so that

$$\vec{F} = m\vec{v}_f = - \int_{-d/2}^{d/2} \mu g \rho \pi a^2 \hat{v}_{re} dl \approx -\mu mg v_{re} \hat{e}_e \quad (26)$$

$$\sum \vec{\tau}_z = I_z \vec{\dot{\omega}}_z = - \int_{-d/2}^{d/2} \vec{l} \times \mu g \rho \pi a^2 \hat{v}_{re} dl - kmg\hat{\omega}_z \approx 0 \quad (27)$$

Assuming that initially  $\theta_z \approx 0$  and  $\omega_z \approx 0$ , the  $y$  component velocity of the rolling object when the contact point is quasistatic is expressed as

$$\vec{y} = \vec{\omega} \times a\hat{k} (1 + \delta) + \Omega\hat{k} \times \vec{y} \approx \vec{\omega} \times a\hat{k} + \Omega\hat{k} \times \vec{y} \quad (28)$$

when  $\delta$  is an infinitesimal. Since  $\theta_z \approx 0$  and rolling friction is negligible compared to the torque applied by kinetic friction,

$$\sum \vec{\tau} = I_l \vec{\dot{\omega}} = amv_f \sin \left( \arctan \frac{\ddot{y}}{\ddot{x}} - \theta_z \right) \hat{l} - \beta m g a \hat{\omega} \approx amv_f \sin \left( \arctan \frac{\ddot{y}}{\ddot{x}} \right) \hat{l} \quad (29)$$

Because  $m\dot{v}_f \sin(\arctan \frac{\ddot{y}}{\ddot{x}})$  is  $y$  component of the net force,

$$m\dot{v}_f \sin\left(\arctan \frac{\ddot{y}}{\ddot{x}}\right) = F_y = m\ddot{y} \quad (30)$$

Using Eq. (28) and Eq. (29), we can arrange the equation about angular acceleration:

$$\vec{\omega} = \frac{am\ddot{y}}{I_l} \hat{l} \quad (31)$$

Combining Eq. (31) and the time derivative of Eq. (28) ( $\dot{\vec{y}} \approx \vec{\omega} \times a\hat{k} + \Omega\hat{k} \times \vec{y}$ ), we can obtain

$$\ddot{\vec{y}} = \frac{I_l}{I_l + ma^2} \Omega\hat{k} \times \dot{\vec{y}} \quad (32)$$

Using the normalized moment of inertia  $I'$ , we can rewrite Eq. (32) as

$$\ddot{\vec{y}} = \frac{I'}{I' + 1} \Omega\hat{k} \times \dot{\vec{y}} \quad (33)$$

Eq. (33) is an equation of an oscillation with angular velocity  $\Omega' = \frac{I'}{I'+1}\Omega$ . Because the circular motion is observed through the rolling motion of the object with contact line, we can conclude that the rolling object executes circular motion with angular velocity  $\Omega' = \frac{I'}{I'+1}\Omega$ , which is analogous to the circular motion of the ball. The transition between the non-slipping stage and slipping stage occurs at  $R_{max}$ , when centrifugal force equates to kinetic friction force as

$$m\Omega'^2 R_{max} = \int_{-d/2}^{d/2} \mu g r \pi a^2 v_{re} dl \approx \mu m g v_{re} \quad (34)$$

Therefore,  $R_{max}$  is approximately expressed as Eq. (16).

### III. COMPUTER SIMULATION

To calculate the trajectory of motion of the rolling object, we use the Ordinary Differential Equation (ODE) solvers in MATLAB. We employ ode 113, which solves non-stiff differential equations by using a variable order method.

By employing Eq. (6) and Eq. (7), we can implement the computer simulation of kinetic friction model for the contact point. By separating the equations using unit vectors, we obtain the following four equations:

$$\ddot{x} = \frac{-\mu g (\dot{x} - a\omega_y + \Omega y)}{\sqrt{(\dot{x} - a\omega_y + \Omega y)^2 + (\dot{y} + a\omega_x - \Omega x)^2}} \quad (35)$$

$$\ddot{y} = \frac{-\mu g (\dot{y} - a\omega_x + \Omega x)}{\sqrt{(\dot{x} - a\omega_y + \Omega y)^2 + (\dot{y} + a\omega_x - \Omega x)^2}} \quad (36)$$

$$\dot{\omega}_x = -\frac{mga}{I} \left( \frac{-\mu (\dot{y} - a\omega_x + \Omega x)}{\sqrt{(\dot{x} - a\omega_y + \Omega y)^2 + (\dot{y} + a\omega_x - \Omega x)^2}} + \frac{\beta\omega_x}{\sqrt{\omega_x^2 + \omega_y^2}} \right) \quad (37)$$

$$\dot{\omega}_y = \frac{mga}{I} \left( \frac{-\mu (\dot{x} - a\omega_y + \Omega y)}{\sqrt{(\dot{x} - a\omega_y + \Omega y)^2 + (\dot{y} + a\omega_x - \Omega x)^2}} - \frac{\beta\omega_y}{\sqrt{\omega_x^2 + \omega_y^2}} \right) \quad (38)$$

Using Eq. (36), Eq. (37), Eq. (38) and Eq. (39), we solve the differential equation using ODE solvers in MATLAB, thereby enabling computer simulations.

The radius of the turntable was set as 5.5m and the angular velocity of the turntable was set as 20rad/s. For convenience, we set the default setting of the rolling object as a ball with a radius 1m and mass 1kg and the initial position as 5m from the center of the turntable. In addition, the default value of the coefficient of rolling friction is 0.01 and default value of the coefficient of kinetic friction is 0.5. We change the dimensionless constants, such as the coefficient of kinetic friction, the coefficient of rolling friction, and the normalized moment of inertia, of the system.

We set the initial velocity to be 0 in the lab frame, the initial motion of the ball to be significantly close to a non-slipping condition, and the initial angular velocity of the ball close to 100rad/s. For convenience purposes, the initial angular velocity of the simulation while changing the coefficient of rolling friction and kinetic friction was 102.5rad/s and the initial angular velocity of the simulation while changing the normalized moment of inertia was 101rad/s.

Simulations while changing the dimensionless constants (coefficient of kinetic friction, coefficient of rolling friction and normalized moment of inertia) were executed in order to observe the various effects that they have on the motion of the rolling object. The simulations while changing the coefficient of rolling friction and kinetic friction was executed for 25 seconds and the simulation while changing the normalized moment of inertia was executed for 50 seconds. The result of the simulations were drawn onto a quarter of the turntable, with the trajectory line of the rolling object represented in Fig. (3)-(8).

From the simulation, it was observed that the frequency of the circular motion, the maximum radius, and the time taken for the transition between the non-slip and slipping condition are independent with the alteration of the coefficient of rolling friction. However,

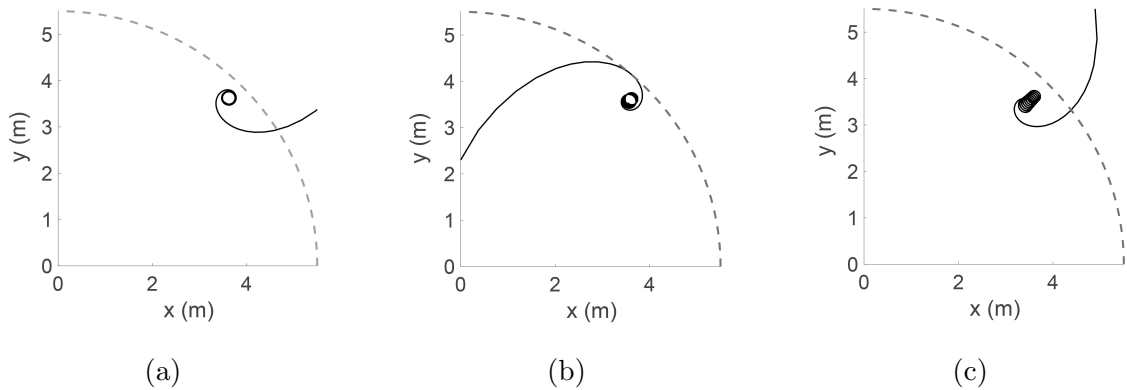


FIG. 3: Computer simulation of the motion while changing the coefficient of rolling friction. The computer outputs are gained through the ODE solver is plotted in the Cartesian coordinate. A quarter of the turntable with its edge is drawn as a dotted curve, and the trajectory of the rolling object, as a solid line, on the graph. The coefficient of rolling friction is (a) 0, (b) 0.01, and (c) 0.03. The simulation is executed for 25 seconds.

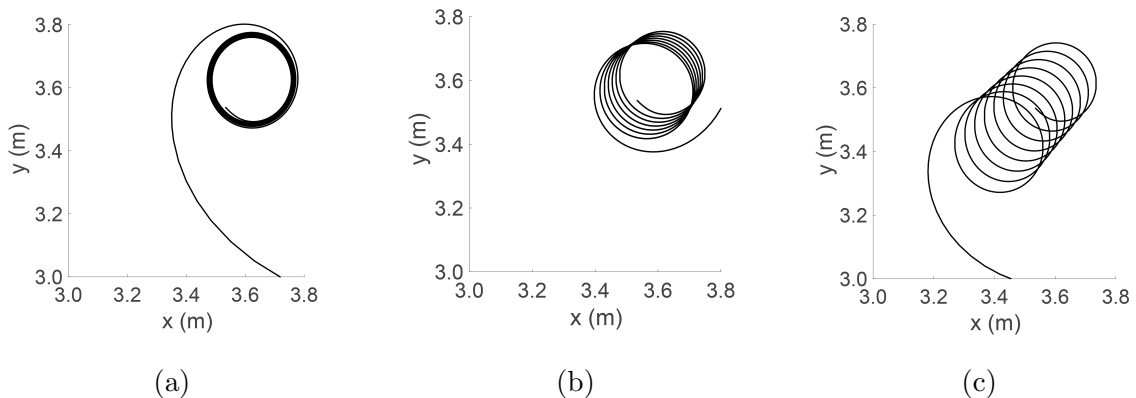


FIG. 4: Magnified image of Fig. 3. The center of the circular motion drifted more towards the center of the turntable, as the coefficient of rolling friction increased.

as the coefficient of rolling friction was increased, the rate of the center of the circular motion drifting towards the center of the turntable increases. When rolling friction is not applied to the system, the circular motion was concentric.

In the system of a rolling ball on a turntable, kinetic friction is the force that enables the circular motion, and can be identified as the main force in the system. According to the simulation, the frequency of the circular motion was independent to the coefficient of kinetic friction in the system. On the other hand, kinetic friction had a close relation to

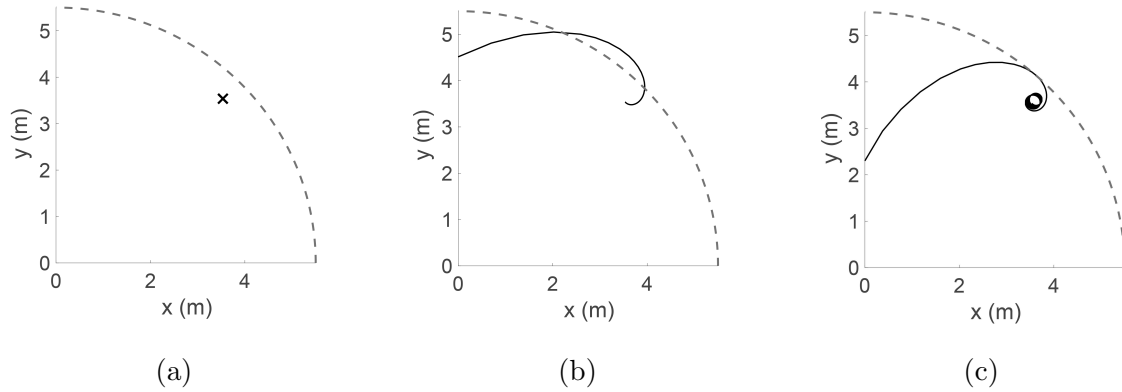


FIG. 5: Computer simulation of the motion while changing the coefficient of kinetic friction. The computer outputs are gained through the ODE solver is plotted in the Cartesian coordinate. A quarter of the turntable with its edge is drawn as a dotted curve, and the trajectory of the rolling object, as a solid line, on the graph. The coefficient of kinetic friction is (a) 0, (b) 0.3, and (c) 0.5. The simulation is executed for 25 seconds.

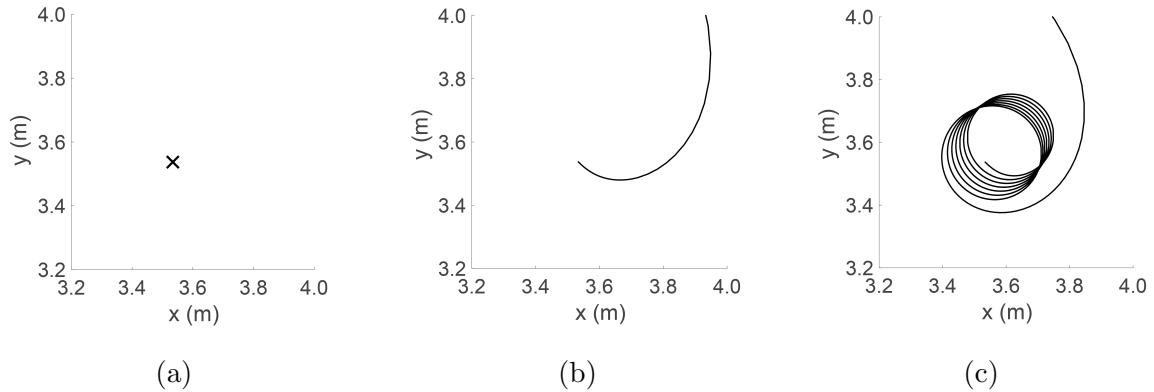


FIG. 6: Magnified image of Fig. 5. The transition between the non-slip and slipping condition took longer as the coefficient of kinetic friction increased.

the transition between the non-slip and slipping condition. Because the transition between rolling with and without slipping occurs when the centrifugal force exceeds the kinetic friction force, the rolling object with a greater coefficient of kinetic friction executes a non-slip motion for a longer period of time and the maximum radius of the orbit increases. The simulations exhibit the transition at the maximum radius of the orbit as theoretically suggested in Eq. (16). As the coefficient of kinetic friction was increased, the rolling object sustained the motion without slipping for longer period.

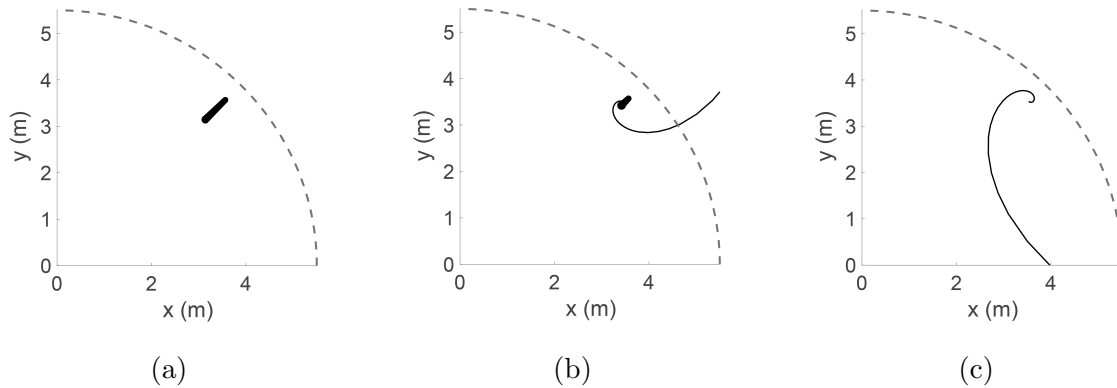


FIG. 7: Computer simulation of the motion while changing normalized moment of inertia.

The computer outputs are gained through the ODE solver is plotted in the Cartesian coordinate. A quarter of the turntable with its edge is drawn as a dotted curve, and the trajectory of the rolling object, as a solid line, on the graph. The normalized moment of inertia is (a)  $2/5$ , (b)  $2/3$ , and (c) 1. The simulation is executed for 50 seconds.

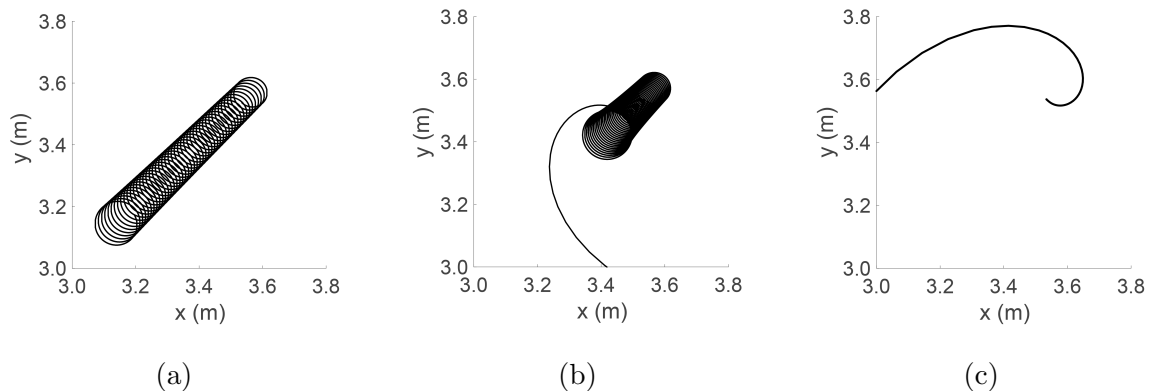


FIG. 8: Magnified image of Fig. 7. The maximum radius before slipping decreased and frequency of the motion increases as normalized moment of inertia increased.

As the normalized moment of inertia increases, maximum radius of the orbit decreases and the frequency of the circular motion, before the transition to slipping motion, increases. The maximum radius of the orbit and frequency of the circular motion analyzed through the simulations follow the suggested model of Eq. (14) and Eq. (16).

The time intervals between the local maxima are equivalent before the ball starts to slip. Therefore, the circular motion without slipping has constant frequency as theoretically solved in Eq. (14). After the maximum radius of the orbit, we can observe that the frequency

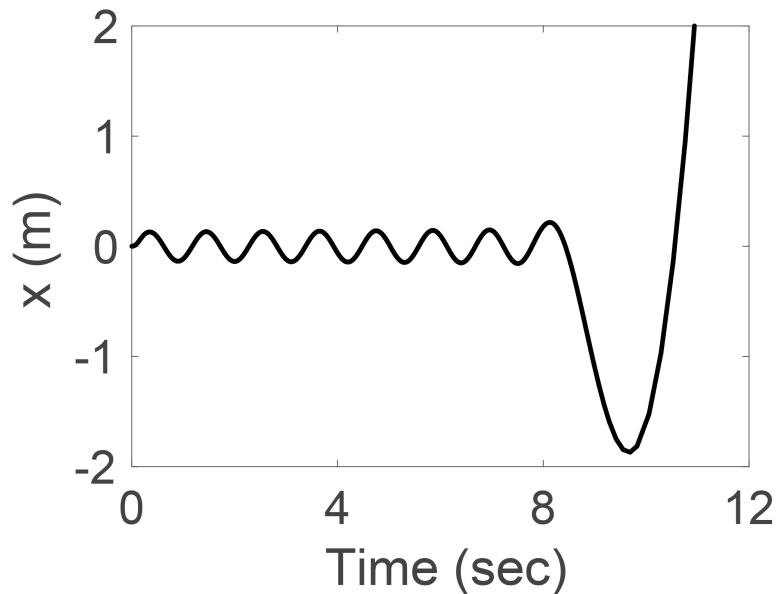


FIG. 9: Computer simulation of x-t graph of the motion. Approximately at 9 second, the frequency of the motion is altered and the distance from the turntable diverges. Before, the frequency of the motion is constant, and the radius of the motion increased gradually.

of the motion changes drastically. The frequency of the motion decreases drastically after the transition between rolling with and without slipping.

The simulation of the kinetic friction model executed a spiral motion with its radius increasing and the center of the circular motion drifting towards the center of the turntable. In addition, after a certain period, the rolling object is expelled from the turntable after it starts slipping. Because the precision of the initial condition is inevitably limited, the simulated trajectory cannot be identical to the experimental trajectory. However, the distance from the center of the turntable to the contact point can be used to measure  $R_{max}$ . The difference of the local maximum and the local minimum, which are adjacent, should be largest before the ball escapes. We define  $R_{max}$  of our computed or measured trajectory as half of the largest difference. We note that our definition correctly reproduces  $R_{max}$  for an ideal circular orbit. The apparent period and frequency of the motion can be obtained by projecting the trajectory onto one dimension of the plane of the turntable.

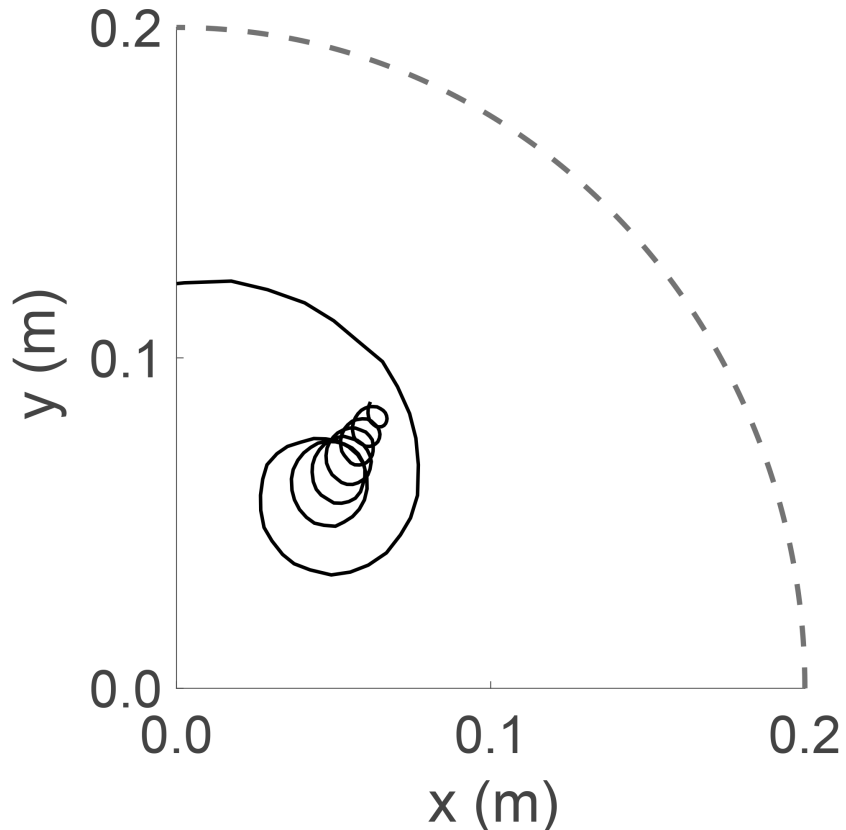


FIG. 10: Observation of the motion. The data was obtained through tracking the ball with the interval of  $1/24$  second. The initial position was  $0.1\text{m}$  from the center of the turntable.

The transition between rolling with and without slipping is observable.

#### IV. EXPERIMENTAL APPROACH

##### A. Methodology

Before the main experiments, we executed preliminary experiments to measure the coefficient of kinetic friction and the normalized moment of inertia. We measured the coefficient of kinetic friction between the rolling object and the surfaces of three different turntables by analyzing the motion of a steel ball without rolling on the inclined plane with an equivalent surface. The coefficient of kinetic friction between the steel ball and the vinyl coated paper is  $0.7194$ , aluminum foil is  $0.7016$ , and the acrylic plate is  $0.6750$ . We measured the normalized moment of inertia of four rolling objects through the analysis of the non-slipping rotating motion of the rolling objects on the inclined plane. The normalized moment of inertia of the

ball is 0.4013, the disc is 0.4412, ring 1 is 0.5812, and ring 2 is 0.6679. We used a turntable of radius 20cm connected to a DC supplier and recorded the motion using video camera (Samsung Electronics, model HMX-S16). We initially fixed the position of the rolling object inside the lab frame to approximately execute a non-slipping rotation. We executed video analysis using software Tracker. We manually measured the maximum radius of the orbit by the method shown above and without slipping and frequency by calculating the difference between the local maxima in the  $x - t$  graph. We did ten experiments per each data points.

### B. Experimental Results

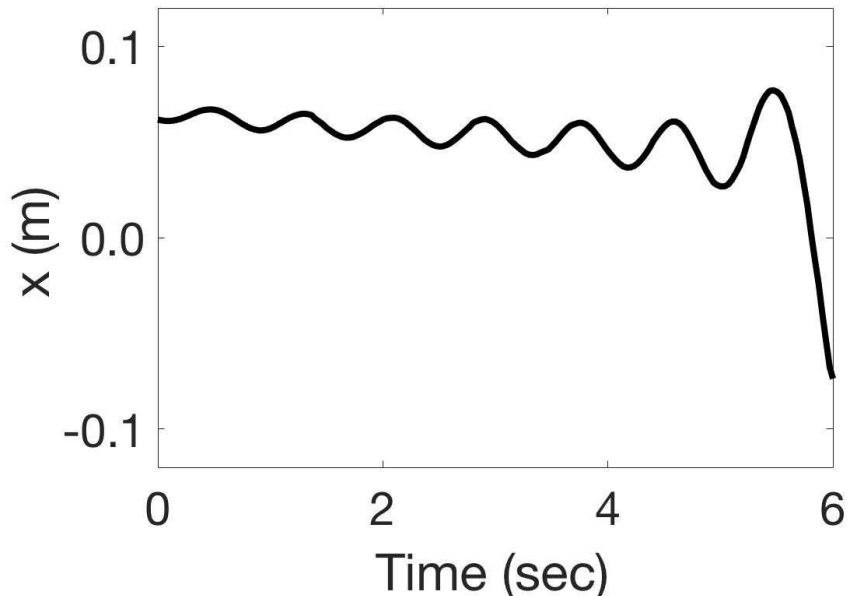


FIG. 11: X time graph of the observed motion. The observation is analogous with the simulation results of Fig. 9. The frequency is approximately constant before the transition between rolling with and without slipping, and the distance from the turntable diverges after the transition.

Although a perfect match of the experimental results and theoretic predictions is impossible due to the inevitably limited precision of initial conditions, the comparison between Fig. 9 and Fig. 11 shows that the characteristics of the motion in both experiments and computer simulations were very similar to each other. The time intervals between the local maxima and the frequency of the motion before the transition between rolling with and

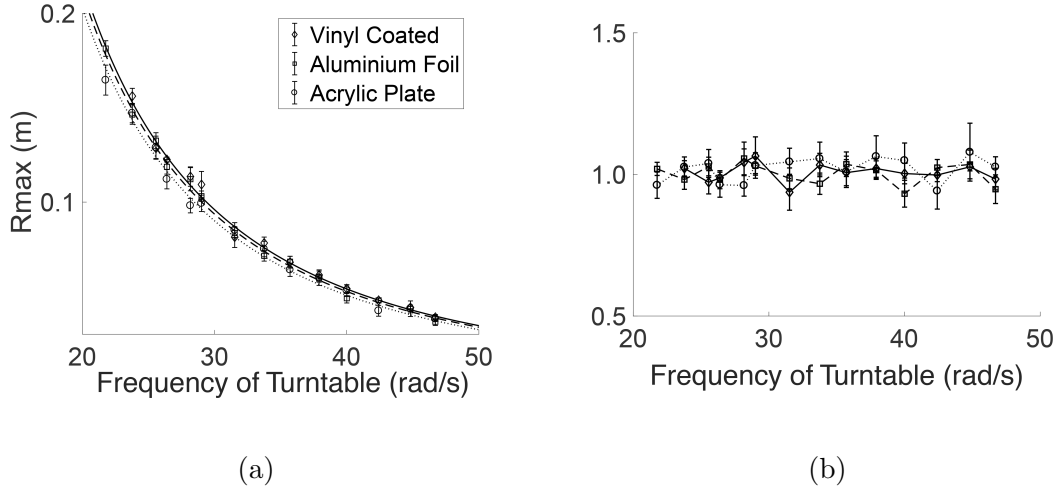


FIG. 12: Experimental data for  $R_{max}$  of the motion of a steel ball with different type of turntable surfaces. The theoretic predictions for  $R_{max}$  of the motion on the vinyl coated turntable is a solid curve, aluminum foil surface is a dashed curve, and the acrylic plate turntable is a dotted curve. The experimental results match the theoretic results from Eq. (16): diamond for the vinyl coated turntable, square for the aluminium foil turntable, and circle for the acrylic plate turntable. In (b), the experimental data are shown as experimental results divided by theoretic predictions.

without slipping are equivalent and follow Eq. (14).

After the transition into a slipping motion, there is a drastic increase in both time intervals between the local maxima and the rate of change in the radius of the motion is observed. Fig. 12 and Fig. 14 show that the experimental data fit very well into the theoretical projections of  $R_{max}$  of the motion from Eq. (16), with the R squared value over 0.97. Fig. 13 shows that the experimental data fits well into the theoretical predictions of the motion based on Eq. (14), with the R squared value over 0.98. Fig. 12 (b) and Fig 14 (b) show that when experimental results are divided by theoretical predictions, the values are evenly distributed near 1. The standard deviation is consistent; the model is equally precise over the range. The tables below show that the actual value is included in the 95% confidence interval, which proves that the actual values of constants are significantly equivalent to the fitted value. From the experiments, it was proven that analyzing the divergent motion assuming that the contact point between the turntable and the rolling object is quasistatic is viable.

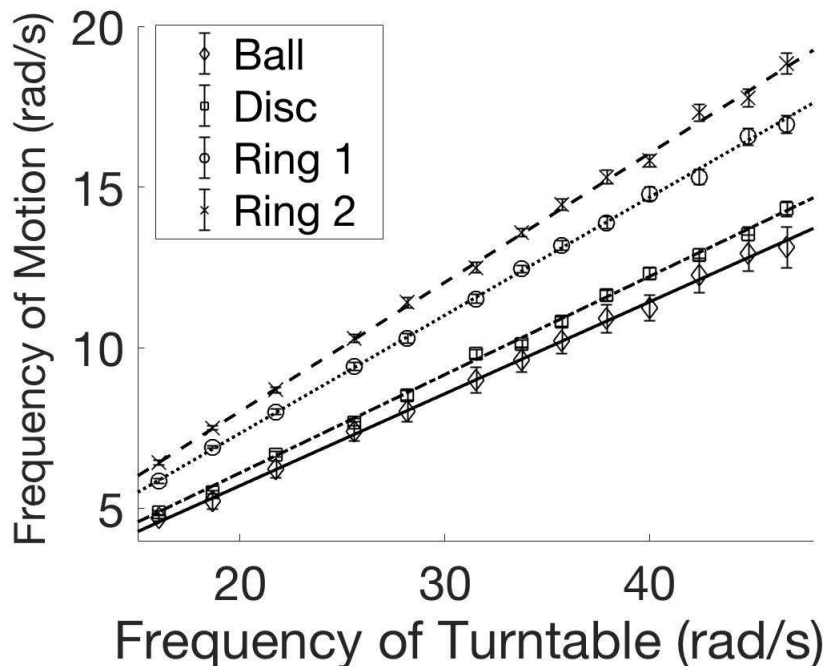


FIG. 13: Experimental data for frequency of the motion on the turntable with acrylic plate surface with various rolling objects. The theoretic predictions for frequency of the motion of the ball is a solid line, disc is a dash-dot line, ring 1 is a dotted line, and ring 2 is a dashed line. The experimental results match the theoretic results from Eq. (14): diamond for ball, square for disc, circle for ring1, and x for ring2.

## V. SUMMARY

The rolling object executes interesting motions when it is placed on a rotating turntable. When the object is initially rolling without slipping, the object executes spiral motion with its radius increasing and the center of the circular motion drifting towards the center of the turntable. After certain period, the motion undergoes transition between rolling with and without slipping. Using kinetic friction model for contact point and line, the motion of the rolling object can be found numerically. Assuming the objects contact point is quasistatic, we approximate the complex motion to circular motion through analyzing maximum radius of the orbit and frequency of the motion.

Kinetic friction model for contact line is the only model that explains the complex dynamics of the disc, ring, and cylinder on the turntable. However, because the model is a complex integro differential equation, the numerical solution is inaccurate and sometimes er-

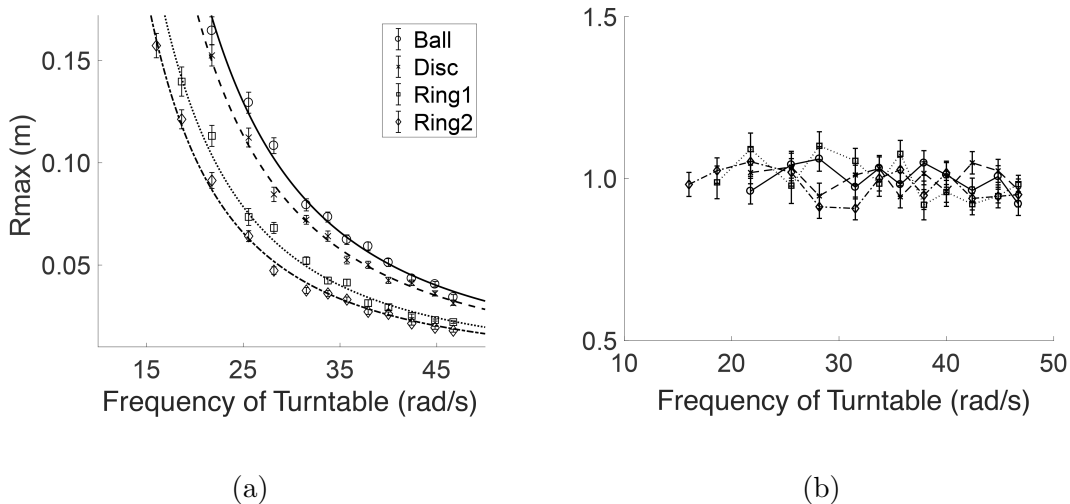


FIG. 14: Experimental data for the  $R_{max}$  of the motion on the turntable with an acrylic plate surface with various rolling objects. The theoretic predictions for the  $R_{max}$  of the motion of the ball is a solid curve, disc is a dashed curve, ring 1 is a dotted curve, and ring 2 is a dash-dot curve. The experimental results match the theoretic results from Eq. (16): circle for ball, x for disc, square for ring1, and diamond for ring2. In (b), the experimental data are shown as experimental results divided by theoretic predictions.

roneous. Through approximation assuming that the rolling object is thin, better theoretical approach is possible.

The novelty of this work is in studying the motion of disc in the dynamics of rolling on the turntable, including its contact line and z axis rotation. An extension to this work would be to execute thorough computer simulation for contact line model and theoretically project the precession of the disc during the motion.

## ACKNOWLEDGMENTS

The authors gratefully acknowledge late professor Myeung Hoi Kwon for constructing turntable which was essential for the experiment.

---

\* davidkm47@gmail.com

Surface of the Turntable	Actual Value	Fitted Value	95% Confidence Interval
Vinyl Coated	0.7194	0.7252	(0.7098, 0.7406)
Aluminium Foil	0.7016	0.7074	(0.6950, 0.7199)
Acrylic Plate	0.6750	0.6772	(0.6607, 0.6936)

(a) Kinetic friction coefficient. Fitted value calculated through curve fitting experimental results of  $R_{max}$  in Fig. 12 (a) with Eq. (16).

Geometry of Rolling Object	Actual Value	Fitted Value	95% Confidence Interval
Ball	0.4013	0.4020	(0.3979, 0.4061)
Disc	0.4412	0.4379	(0.4336, 0.4423)
Ring 1	0.5812	0.5788	(0.5739, 0.5837)
Ring 2	0.6679	0.6715	(0.6641, 0.6789)

(b) Normalized moment of inertia. Fitted value calculated through curve fitting experimental results of frequency of the motion in Fig. 13 with Eq. (14).

Geometry of Rolling Object	Actual Value	Fitted Value	95% Confidence Interval
Ball	0.4013	0.3996	(0.3915, 0.4078)
Disc	0.4412	0.4377	(0.4305, 0.4448)
Ring 1	0.5812	0.5709	(0.5551, 0.5867)
Ring 2	0.6679	0.6709	(0.6580, 0.6838)

(c) Normalized moment of inertia. Fitted value calculated through curve fitting experimental results of  $R_{max}$  in Fig. 14 (a) with Eq. (16).

TABLE II: The comparison between the actual value and the fitted value obtained from curve fitting the experimental results. In (a), we compared the actual value and the fitted value of the kinetic friction coefficient between the steel ball and the turntable. In (b) and (c), we compare the actual value and the fitted value of the normalized moment of inertia of the rolling objects.

<sup>†</sup> johnnlee24@gmail.com

<sup>‡</sup> donggeonoh1999@gmail.com

<sup>§</sup> yyoon@cau.ac.kr

<sup>¶</sup> copark@gachon.ac.kr

- <sup>1</sup> Klaus Weltner, “Stable circular orbits of freely moving balls on rotating discs,” *Am. J. Phys* **47** (11), 984–986 (1979).
- <sup>2</sup> Klaus Weltner, “Central drift of freely moving balls on rotating disks: A new method to measure coefficients of rolling friction,” *Am. J. Phys* **55** (10), 937–942 (1987).
- <sup>3</sup> Joel Gersten, Harry Soodak, and Martin S. Tiersten, “Ball moving on stationary or rotating horizontal surface,” *Am. J. Phys* **60** (1), 43–47 (1992).
- <sup>4</sup> Warren Weckesser, “A ball rolling on a freely spinning turntable,” *Am. J. Phys* **65** (8), 736–738 (1997).
- <sup>5</sup> Artjom V. Sokirko, Alexandr A. Belopolskii, Andrei V. Matytsyn, and Dmitri A. Kossakowski, “Behavior of a ball on the surface of a rotating disk,” *Am. J. Phys* **62** (2), 151–156 (1994).
- <sup>6</sup> Robert Ehrlich, Jaroslaw Tuszynski, “Ball on a rotating turntable: comparison of theory and experiment,” *Am. J. Phys* **63** (4), 351–359 (1995).
- <sup>7</sup> Akshat Agha, Sahil Gupta, and Toby Joseph, “Particle sliding on a turntable in the presence of friction,” *Am. J. Phys* **82** (2), 126–132 (2015).
- <sup>8</sup> Harry Soodak, Martin S. Tiersten, “Perturbation analysis of rolling friction on a turntable,” *Am. J. Phys* **64** (9), 1130–1139 (1996).
- <sup>9</sup> Daolin Ma, Caishan Liu, Zhen Zhao, and Hongjian Zhang, “Rolling friction and energy dissipation in a spinning disc,” *Proc. R. Soc. A* **470** (2169), DOI: 10.1098(2014).
- <sup>10</sup> John H. Jellett, *A Treatise on the Theory of Friction* (Hodges, Foster, and Company, 1872)
- <sup>11</sup> A. V. Borisov, I. S. Mamaev, A. A. Kilin, “Dynamics of rolling disk,” *Regul. Chaotic Dyn* **8** (2), 201–212 (2003).
- <sup>12</sup> O. M. O’Reilly, “The dynamics of rolling disks and sliding disks,” *Nonlinear Dyn* **10** (3), 287–305 (1996).
- <sup>13</sup> Ju. I. Neimark, and N. A. Fufaev *Dynamics of Nonholonomic Systems* (American Mathematical Society, 2004)
- <sup>14</sup> R. I. Leine, “Experimental and theoretical investigation of the energy dissipation of a rolling disk during its final stage of motion,” *Arch. Appl. Mech* **79** (11), 1063–1082 (2009).
- <sup>15</sup> C. Le Saux, R. I. Leine, and C. Glocker, “Dynamics of a rolling disk in the presence of dry friction,” *J. Nonlinear Sci* **15** (1), 27–61 (2005).

- <sup>16</sup> Z. Farkas, G. Bartels, T. Unger, and D. E. Wolf, “Frictional coupling between sliding and spinning motion,” *Phys. Rev. Lett* **90** (24), 248302 (2003).
- <sup>17</sup> P. D. Weidman, and C. P. Malhorta, “Regimes of terminal motion of sliding spinning disks,” *Phys. Rev. Lett* **95** (26), 264303 (2005).
- <sup>18</sup> D. G. FLoM, and A. M. Bueche, “Theory of rolling friction for spheres,” *J. Appl. Phys* **30** (11), 1725–1730 (1959).
- <sup>19</sup> D. Tabor, “CV. The mechanism of rolling friction,” *Edinb.Dubl.Phil.Mag* **43**(345), 1055–1059 (1952).
- <sup>20</sup> K. Kendall, “Rolling friction and adhesion between smooth solids,” *Wear* **33**(2), 351–358 (1975).
- <sup>21</sup> A. Domenech, T. Domenech, and J. Cebrian, “Introduction to the study of rolling friction,” *Am. J. Phys* **55**(3), 231–235 (1987).